

Joint Cutting for Hybrid Schrödinger-Feynman Simulation of Quantum Circuits

Laura S. Herzog[†], Lukas Burgholzer^{†§}, Christian Ufrecht[‡], Daniel D. Scherer[‡], Robert Wille^{†§¶}

[†] Chair for Design Automation, Technical University of Munich, Germany

[‡] Fraunhofer Institute for Integrated Circuits IIS, Nuremberg, Germany

[§] Munich Quantum Software Company GmbH, Garching near Munich, Germany

[¶] Software Competence Center Hagenberg GmbH (SCCH), Hagenberg, Austria

Abstract—Despite the continuous advancements in size and robustness of real quantum devices, reliable large-scale quantum computers are not yet available. Hence, classical simulation of quantum algorithms remains crucial for testing new methods and estimating quantum advantage. Pushing classical simulation methods to their limit is essential, particularly due to their inherent exponential complexity. Besides the established *Schrödinger-style* full statevector simulation, so-called *Hybrid Schrödinger-Feynman* (HSF) approaches have shown promise to make simulations more efficient. HSF simulation employs the idea of “cutting” the circuit into smaller parts, reducing their execution times. This, however, comes at the cost of an exponential overhead in the number of cuts. Inspired by the domain of Quantum Circuit Cutting, we propose an HSF simulation method based on the idea of “joint cutting” to significantly reduce the aforementioned overhead. This means that, prior to the cutting procedure, gates are collected into “blocks” and all gates in a block are jointly cut instead of individually. We investigate how the proposed refinement can help decrease simulation times and highlight the remaining challenges. Experimental evaluations show that “joint cutting” can outperform the standard HSF simulation by up to a factor $\approx 4000\times$ and the Schrödinger-style simulation by a factor $\approx 200\times$ for suitable instances. The implementation is available at <https://github.com/cda-tum/mqt-qsim-joint-cutting>.

Index Terms—quantum computing, classical simulation, hybrid Schrödinger-Feynman, joint cutting, circuit cutting

I. INTRODUCTION

As the availability of reliable large-scale, fault-tolerant quantum computers is still pending, classical simulation of quantum circuits remains a central tool for quantum computing research—including developing and testing quantum algorithms as well as comparing classical computers against current quantum hardware. Such simulations are inherently challenging due to the exponential scaling of the statevectors’ dimension with a growing number n of qubits. The standard approach for quantum circuit simulation is the so-called *Schrödinger-style* simulation which directly applies the quantum gates on the full statevector via matrix-vector multiplication. As this requires storing a vector with 2^n entries, storage capacities are quickly exhausted. Additionally, the runtimes increase heavily with growing n . Even though the exponential scaling cannot be avoided, any decrease in memory and runtime is desirable.

Hybrid Schrödinger-Feynman (HSF) [1]–[3] techniques tackle this by trading memory complexity for time complexity. This is done by partitioning large circuits into smaller subcircuits, e.g., with $\lceil n/2 \rceil$ qubits each. However, such partitioning

requires “cutting” gates that connect the different partition which generates multiple, smaller, subcircuits to be simulated. With an increasing number of cuts, also the number of subcircuits grows exponentially. This count of smaller subcircuits, so-called “paths”, is thus determined by the chosen quantum algorithm to be simulated—allowing faster runtimes as long as the circuit’s cut induces only a reasonable number of paths.

The state-of-the-art HSF technique applies such “cuts” separately on each gate to be cut. We propose enhancing this procedure by, first, grouping the gates to be cut and, then, performing a “joint cut” on the grouped gates. Gates can be cut jointly by multiplying the respective gates and performing a Schmidt Decomposition afterwards—while this can be done automatically, one can also find analytical expressions for specific cut blocks. For certain classes of quantum circuits, the proposed method not only speeds up simulation runtimes compared to standard HSF computations but also extends the HSF simulation’s applicability to instances where standard Schrödinger-style simulation would otherwise have been faster.

The remainder of this paper is structured as follows. In Sec. II the necessary basics about quantum computing and quantum circuit simulation as well as the concepts behind HSF simulation are detailed. Afterwards, in Sec. III, we introduce the idea of “joint cutting” and review related work. Following up on this, Sec. IV provides important details about the realization of the proposed idea along with practical considerations. Finally, the results obtained during the evaluation of the proposed approach are summarized in Sec. V and the paper is concluded in Sec. VI.

II. BACKGROUND

To keep this paper self-contained, this section reviews the basic nomenclature of quantum circuits, the core ideas of quantum circuit simulation on classical computers, and the essential concepts of Hybrid Schrödinger-Feynman simulation.

A. Quantum Circuits and Schrödinger-style Simulation

An n -qubit quantum system can be described by its *statevector*, an element of a Hilbert space $\mathcal{H}_2^{\otimes n}$, where the Hilbert space of a single qubit is $\mathcal{H}_2 = \text{span}(\{|0\rangle, |1\rangle\})$. Thus, the dimension of this space scales exponentially with the number n of qubits in the considered quantum system—leading to inevitable limits regarding storing such vectors on

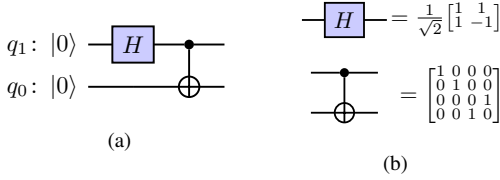


Fig. 1: Quantum circuit (a) and the corresponding gates (b) for a Bell state preparation.

classical machines. In Dirac notation, a state $|\psi\rangle$ residing in this space can be written as

$$|\psi\rangle = \sum_{i \in \{0,1\}^n} \psi_i |i\rangle, \quad (1)$$

with the amplitudes $\psi_i \in \mathbb{C}$ and $i = (i_{n-1}, \dots, i_0) \in \{0,1\}^n$. The qubits' state can be manipulated by applying quantum gates, which are described as unitary operators acting on the Hilbert space. Representing the operator in the computational basis, the output state after application of the corresponding gate can be determined by applying matrix-vector multiplication. Performing this procedure of consecutive matrix-vector multiplications on a classical computer is the core idea of *Schrödinger-style* simulation. We refer to [4] for a broader review.

Example 1. Consider the quantum circuit shown in Fig. 1a. The computation starts with the all-zero statevector for two qubits with $2^2 = 4$ entries, i.e.,

$$|00\rangle = |0\rangle \otimes |0\rangle = [1, 0]^T \otimes [1, 0]^T = [1, 0, 0, 0]^T. \quad (2)$$

Following the circuit, a Hadamard and a CNOT gate are applied, whose matrix representations are shown in Fig. 1b. Directly performing the consecutive matrix-vector multiplication on $|00\rangle$ leads to the state

$$(\text{CNOT} \cdot ((H \otimes I) |00\rangle)) = \frac{1}{\sqrt{2}} \cdot [1, 0, 0, 1]^T, \quad (3)$$

with I being the 2×2 identity matrix. The result corresponds to the well-known Bell state $|\Phi\rangle^+ = \frac{1}{\sqrt{2}}(|00\rangle + |11\rangle)$.

Classical simulation of quantum circuits, as reviewed above, can be performed by employing different data structures for representing the exponential number of amplitudes in the statevector. Directly following the treatment in Ex. 1, one can use plain arrays to store the statevector, matrix representations of gates, and for performing matrix-vector multiplication. Alternative structures have been investigated to cope with the exponential complexity. Examples include *tensor networks* [5]–[8] which emerged from the field of condensed matter physics as well as *Decision Diagrams* (DDs) originating from the *Electronic Design Automation* (EDA) community [9]–[12].

In addition to various data structures, alternative simulation schemes to standard Schrödinger-style simulation exist, as its major issue is storing and handling the exponentially large statevector. A prominent method that tackles this weakness, *Hybrid Schrödinger-Feynman* (HSF) simulation, is reviewed next.

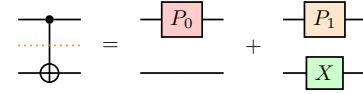


Fig. 2: Bipartite representation of the CNOT gate. The orange, dotted line indicates the “cut”.

B. Hybrid Schrödinger-Feynman Simulation

HSF simulation [1]–[3] aims to reduce the inherent exponential memory complexity involved in classically simulating quantum circuits—at the expense of exponential runtime. The idea of HSF simulation is to horizontally partition the circuit into, for instance, two subcircuits with a similar number of qubits. This reduces the memory complexity, e.g., from $\mathcal{O}(2^n)$ to $\mathcal{O}(2^{\lceil n/2 \rceil})$, assuming a partitioning into two subcircuits with $\approx n/2$ qubits each. Since a fraction of gates usually acts across both partitions, this procedure requires “cutting” those connecting gates. This needs a factorized representation of the gate that ensures its constituents only act locally on their partition. The following example illustrates the idea.

Example 2. Consider the CNOT gate as an example. Finding a bipartite representation of the CNOT gate can be easily done by factoring out properly, i.e.,

$$\text{CNOT} = |0\rangle\langle 0| \otimes I + |1\rangle\langle 1| \otimes X = P_0 \otimes I + P_1 \otimes X.$$

An illustration of this factorization is provided in Fig. 2. Thus, a CNOT gate can be directly decomposed into two terms composed of local unitaries only.

To find such bipartite representations more generally, one can perform a *Schmidt Decomposition* [4] of the corresponding unitary. As will be explained in more detail in Sec. IV, the Schmidt Decomposition allows to find representations of the form

$$A = \sum_{m=0}^{r-1} \sigma_m X_m \otimes Y_m, \quad (4)$$

for arbitrary operators $A : \mathcal{H}_2^{\otimes n_a} \rightarrow \mathcal{H}_2^{\otimes n_b}$. The matrix of X_m is of size $2^{n_a} \times 2^{n_a}$ while Y_m is of size $2^{n_b} \times 2^{n_b}$ such that $n_a + n_b = n$ holds. The value r is denoted as the *Schmidt-rank* and σ_m are the singular values.

Thus, one can find a bipartition to perform a cut for general n -qubit gates. Each term of the Schmidt-decomposed gate constitutes a pair of circuits to be simulated separately—each pair being a “path” in the overall simulation. If all gates connecting the two partitions are cut, one receives a set of smaller subcircuits, such that their memory complexity can be reduced, e.g., from 2^n to $2^{\max(n_a, n_b)}$. This reduced memory complexity then also reduces the overall runtime. The number of elements in this set, however, scales exponentially with the number of gates being cut. This leads to an overhead in time complexity, which can partly be remedied by parallel simulation of the numerous paths. The final result is reconstructed by applying the Kronecker product between the subcircuits per simulation and adding up all contributions.

The HSF technique is named for its hybrid approach, combining Schrödinger-style simulation (using matrix-vector multiplication for subcircuits) with Feynman-style simulation

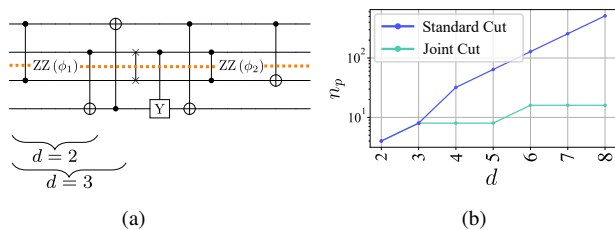


Fig. 3: (a) An exemplary circuit of which different depths d are considered. For $d = 2$ only the two leftmost gates are included and so on. The dotted, orange line indicates the location of the cut. (b) For different depths d , the number of paths n_p increases more rapidly with standard cutting compared to joint cuts, which saturate. The steeper slope from $d = 3$ to $d = 4$ for standard cutting is due to the SWAP gate’s Schmidt rank $r = 4$, whereas the others have $r = 2$.

that explores different “paths”. Although a full Feynman-style simulation, i.e., cutting *all* multi-qubit gates, is computationally impractical, the hybrid method has proven quite effective.

III. MOTIVATION AND GENERAL IDEA

The main strength of the HSF simulation is to reduce the memory complexity by partitioning the circuit into smaller parts. However, this comes with a cost: The more gates are cut during the partitioning, the more paths have to be simulated. Generally, the number n_p of paths scales exponentially with the number of cuts. If m gates are cut, one has $n_p = \prod_{i=0}^{m-1} r_i$ paths where r_i is the Schmidt-rank of each cut gate. If all gate decompositions have the same rank r , one can simplify this to $n_p = r^m$. Thus, not every quantum circuit is suitable for being simulated with HSF approaches: Even with parallelization of the different paths, the exponentially increasing n_p quickly renders the runtime prohibitive. Hence, the HSF simulation offers advantages for shallow circuits and circuits that can be partitioned into weakly connected sections—allowing for a sweet spot in the trade-off between reduced memory usage and the increased number of paths.

However, in this work we show that the full potential of HSF simulation has not been reached yet. Reducing n_p is possible by going beyond the naive approach of cutting each gate separately. In this work, we propose to perform “joint cuts” by forming suitable groups of gates in the circuit first and cutting them jointly with a Schmidt Decomposition. After illustrating how this procedure can be exploited in principle, the connections of our work and the related field of Quantum Circuit Cutting (QCC) [13]–[19] will be briefly reviewed.

A. Reducing the Number of Paths with “Joint Cutting”

As mentioned above, individually applying cuts to each gate that connects multiple partitions directly results in an exponentially growing number n_p of paths. While this exponential scaling cannot be completely avoided, there is some flexibility in the way gates are cut. For instance, if several gate cuts can be grouped, i.e., *jointly* cut, the number n_p of paths can be reduced considerably. An example illustrates the effect.

Example 3. Consider the circuit to be simulated as shown in Fig. 3a and assume a partitioning that leads to a subcircuit with qubits q_0 and q_1 as well as one with qubits q_2 and q_3 . In a straightforward application of HSF simulation, one

performs a Schmidt decomposition on every single gate on the cut, such that n_p is the product of all separate Schmidt-ranks. Instead, we can combine the gates first and then cut them jointly by performing a Schmidt Decomposition of the resulting unitary. The behavior of n_p in these cases is summarized in Fig. 3b, where n_p is plotted for increasing depths d of the example circuit from Fig. 3a. This clearly shows the potential of the “joint cutting” approach for which the number of paths saturates at $n_p = 2^{2 \cdot 2} = 16$ while the state-of-the-art cutting scheme scales exponentially with d .

While this example was artificially created to demonstrate the potential benefits, our experimental evaluations, which are summarized later in Sec. V, show the practical advantage of the proposed “joint cutting” scheme.

The number n_p of paths is reminiscent of a corresponding quantity within the field of *Quantum Circuit Cutting* (QCC), which is briefly reviewed in the next section.

B. Related Work

An advantageous aspect of (joint) cutting for quantum circuit simulation is that the *Singular Value Decomposition* (SVD) can be found for any matrix, and therefore the Schmidt Decomposition (Sec. IV-A) can always be constructed. Thus, the cuts can be performed fully automatically, even though it is also possible to find analytical decompositions as demonstrated in Sec. IV-D. HSF simulation techniques enjoy further freedom since the decomposition does not need to correspond to quantum operations, hence do not need to be unitary, such as the projectors P_0, P_1 from Ex. 2. Changing the point of view regarding the treatment of algorithms on real quantum devices, cutting can be performed as well, but in a more constrained manner.

QCC aims to partition quantum circuits such that they can be run on smaller quantum computers. Hence, QCC and HSF approaches stem from the same core idea: Circumventing the effects of limited memory—be it RAM on a classical computer or the number of qubits in a quantum computer. Additionally, QCC can also help to reduce the impact of noise on current NISQ devices [20]. Though both fields are related, decomposing gates in a QCC framework differs notably from the Schmidt decomposition applied in HSF simulations. In contrast to the aspects mentioned above, finding a decomposition for individual or combined gates cannot be done automatically and necessitates detailed, manual examination on a case-by-case basis.

More formally, in QCC the quantum channel of the gate is decomposed, in contrast to HSF simulation, where we decompose the matrix representing the gate. More specifically, in QCC, the decomposition takes the form of a *Quasi-Probability Decomposition* (QPD) $\mathcal{W} = \sum_i a_i \mathcal{F}_i$. Each of the \mathcal{F}_i is a bipartite channel, where operations are applied independently to each partition without connecting them, similar to the illustration in Fig. 2. The QPD is realized on a quantum computer by sampling the operation \mathcal{F}_i with probability proportional to $|a_i|$ and recombining the results by classical postprocessing. This procedure comes with a *sampling overhead* which scales exponentially with the number of cuts. Note that the number of \mathcal{F}_i ’s is reminiscent of the number n_p of paths in the

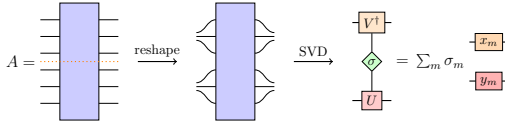


Fig. 4: Illustration of reshaping the matrix of A and performing an SVD.

HSF simulation and also scales exponentially with the number of cuts in the case of QCC. An endeavor in QCC is to reduce both the number of \mathcal{F}_i 's as well as the aforementioned sampling overhead. Even though the exponential scaling cannot be avoided, it can be remedied to some extent by introducing “joint cutting” [18], [21]–[23] for QCC. Similar to the proposed “joint cutting” for HSF simulation, in QCC, multiple gates are combined and, while exploiting the resulting structure, more beneficial decompositions can be found.

IV. TECHNICAL DETAILS

In the following, we will elaborate on the ideas proposed above and illustrated in Ex. 3, i.e., how the Schmidt Decomposition is performed on general (blocks of) gates and why we can reach a saturation in n_p . Furthermore, we point out that the overhead from the Schmidt Decomposition can become significant and how “joint cutting” can be used in practice.

A. General Schmidt Decomposition

The core idea of the Schmidt Decomposition is to perform a *Singular Value Decomposition* (SVD) and to rotate the basis as illustrated in Fig. 4. As indicated in the figure, one can reshape the qubit wires (interpreted as legs of the corresponding tensor) according to the cut (orange dotted line). Afterwards, the SVD is performed which constitutes a bipartite representation. Mathematically speaking, each quantum gate is an operator acting on the qubits’ Hilbert space. Given an operator $A : \mathcal{H}_2^{\otimes n} \rightarrow \mathcal{H}_2^{\otimes n}$ with n qubits, it can be written as

$$A = \sum_{i,j \in \{0,1\}^n} A_{i,j} |i\rangle \langle j|, \quad (5)$$

where $i = (i_{n-1}, \dots, i_0)$ and $j = (j_{n-1}, \dots, j_0)$. The coefficients $A_{i,j}$ can be regarded as a 2^{2n} -dimensional object. We want to decompose the unitary into partition a and b with the indices $i^a = (i_{n-1}, \dots, i_{l+1})$, $i^b = (i_l, \dots, i_0)$ and equivalently for j^a and j^b . Thus, the cut is performed between qubit l and $l+1$. This requires reshaping and matricization, i.e.,

$$A = \sum_{\mathbf{i}_{\leq l}, \mathbf{i}_{> l}} \tilde{A}_{\mathbf{i}_{\leq l}, \mathbf{i}_{> l}} |i^a\rangle \langle j^a| \otimes |i^b\rangle \langle j^b|, \quad (6)$$

with $\mathbf{i}_{\leq l} = (i^b, j^b)$ and $\mathbf{i}_{> l} = (i^a, j^a)$ as well as $\tilde{A}_{\mathbf{i}_{\leq l}, \mathbf{i}_{> l}}$ is a relabeled $A_{i,j}$. Now, the SVD can be applied such that

$$\tilde{A}_{\mathbf{i}_{\leq l}, \mathbf{i}_{> l}} = \sum_{m=0}^{r-1} U_{\mathbf{i}_{\leq l}, m} \sigma_m V_{m, \mathbf{i}_{> l}}^*, \quad (7)$$

with the *Schmidt-rank* r . The U and V^* can be absorbed in the basis as

$$X_m = \sum_{\mathbf{i}_{> l}} V_{m, \mathbf{i}_{> l}}^* |i^a\rangle \langle j^a| \quad (8)$$

$$Y_m = \sum_{\mathbf{i}_{\leq l}} U_{\mathbf{i}_{\leq l}, m} |i^b\rangle \langle j^b|, \quad (9)$$

leading to a bipartite representation of the original matrix of A shown in Eq. 4.

B. Theoretical Guarantee for Lower n_p

In general, it is known that the Schmidt-rank of a matrix is limited by its dimension. This means that the matrix of an operator $A : \mathcal{H}_2^{\otimes n} \rightarrow \mathcal{H}_2^{\otimes n}$ of a block with n qubits which is split into partitions with n_a, n_b qubits, respectively, can have a Schmidt-rank at most $\tilde{r} = \min(2^{2n_a}, 2^{2n_b})$ [24]. This behavior is the explanation for the saturation of n_p for the “joint cutting” in Ex. 3: While this bound applies individually to each cut gate when applied consecutively, it does not hold collectively for all gates. In contrast, for joint gate cutting, the limit applies to the entire block—leading to the aforementioned saturation of $2^{2 \cdot 2}$. Therefore, “joint cutting” is guaranteed to reduce n_p for deep enough blocks with limited dimensions.

To illustrate this in mathematical terms, consider a sequence of operators $\mathcal{N} = \{A_k\}_{k=0}^{K-1}$ where $A_k : \mathcal{H}_2^{\otimes n} \rightarrow \mathcal{H}_2^{\otimes n}$. They are cut into partitions with n_a, n_b qubits respectively. The “joint cutting” is guaranteed to reduce n_p as soon as

$$n_p^t = \prod_{k=0}^{K-1} r_k > \tilde{r} \geq n_p^j \quad (10)$$

holds, where r_k denotes the Schmidt-rank of the matrix of A_k . The left-hand side comes from multiplying up all Schmidt-ranks within \mathcal{N} for the standard cutting, leading to n_p^t paths. On the other hand, the maximum number of “joint cutting” paths, n_p^j , is upper bounded by \tilde{r} , i.e., the smaller dimension of the reshaped matrix on which the SVD is performed (Eq. 7).

One should note, however, that in Ex. 3, already before the saturation of n_p , the “joint cutting” reduces n_p in comparison to the standard cutting. Thus, the above guarantee does not need to be exhausted to make “joint cutting” for HSF simulations beneficial.

C. Overhead for “Joint Cutting”

Joining gates into blocks for “joint cutting” comes with a cost that has to be drawn into consideration regarding the usefulness of the proposed “joint cutting” technique. In general, merging a block of gates into one requires consecutive matrix multiplications first and afterwards a Schmidt Decomposition. The first usually has the asymptotic time complexity $\mathcal{O}(D^s)$ with $2 \leq s \leq 3$ and the SVD within the latter $\mathcal{O}(D^3)$. Here, $D = 2^k$ for a k -qubit block, and therefore including too many qubits in a block in relation to the whole circuit can make “joint cutting” ineffective—unless analytical decompositions can be found (Sec. IV-D).

Therefore Ex. 3 may have a reduced number of paths n_p but the preprocessing would dominate the total simulation runtime. Strictly speaking, the preprocessing is more costly than direct Schrödinger simulation, as the latter primarily involves matrix-vector multiplication ($\mathcal{O}(D^2)$). As a consequence, “joint cutting” can only be useful if utilized with care: Joining only a few gates in a large circuit can severely decrease the number of paths n_p . If small enough blocks are chosen, one receives the best of both worlds: A reduction in n_p as well as negligible preprocessing overhead.

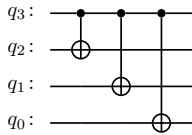


Fig. 5: A “cascade” of CNOT gates.

D. “Joint Cutting” in Practice

In practice, it is recommended to consider quantum circuits following a beneficial structure for “joint cutting”. One such structure is “cascades” of two-qubit gates.

Example 4. Consider Fig. 5 in which an example cascade of CNOT gates is displayed. Referring to the decomposition of the CNOT gate in Ex. 2, one can deduce the decomposition of the cascade of three CNOT gates $C_{\text{CNOT},3}$ as

$$C_{\text{CNOT},3} = P_0 \otimes I \otimes I \otimes I + P_1 \otimes X \otimes X \otimes X. \quad (11)$$

Thus, the Schmidt-rank remains $r = 2$, such that a joint cut of this structure would be much smarter than standard cutting with $n_p^t = 2^3$.

This structure is also beneficial for different kinds of gates such as, for instance, CZ or RZZ gates—which occur in many quantum algorithms.

V. EXPERIMENTAL EVALUATION

To evaluate the performance of the proposed “joint cutting” method for HSF simulations, we built upon Google’s qsim package [25], a high-performant array-based quantum simulator used for cross-entropy benchmarking in [26]. The “joint cutting” implementation is open-source and available at <https://github.com/cda-tum/mqt-qsim-joint-cutting>. All evaluations were performed on a machine with a 16-core AMD Ryzen Threadripper PRO 5955WX CPU and 128 GB RAM. To keep the computation times reasonably low while still considering instances of relevant size, only a fraction of the total amplitudes (10^6) was computed for all considered methods.

As a case study, we look at quantum algorithms for solving *Quadratic Unconstrained Binary Optimization* (QUBO) problems, which, at the time of writing, arguably constitute the largest area of research when it comes to applications of quantum computing. In particular, we consider the *Quantum Approximate Optimization Algorithm* (QAOA) for solving the Max Cut problem, as it has been shown that any QUBO problem can be reduced to a weighted Max Cut instance [27]–[30]. The circuits consist of multiple alternating so-called *problem* and *mixer* layers, for which one uses RZZ entangling gates as well as single-qubit RX rotation gates, respectively. RZZ gates mutually commute, which gives a lot of freedom to reorder the gates such that grouping and, therefore, “joint cutting” can be performed—see Fig. 6 for an example.

To control the number of gates to cut for the HSF simulation, we considered graphs with two partitions of nodes with roughly the same size and place the cut between the partitions. Nodes are connected with probability p_{intra} within the partition and with, usually lower, probability p_{inter} between the partitions. Note that an original, denser, problem graph could

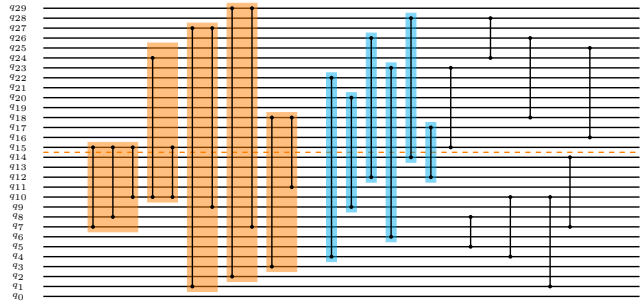


Fig. 6: Examples of RZZ gates of a problem layer in QAOA from a graph with 15 qubits per partition (q30-1). The orange dotted line denotes the cut and the orange shaded gates are the utilized blocks. Blue shaded gates are cut separately. Only a few of the uncut gates are displayed without coloring.

be shrunk to an instance that is easier to execute [31]. Given the cut location, we use a brute force algorithm to reassemble cascades of RZZ gates which can be cut jointly. To keep the implementation more general, the joint cuts were performed numerically, even though analytical expressions can be found for “cascade” structures as shown in Ex. 4.

Tab. I summarizes the results of evaluating qsim’s Schrödinger Simulation, its standard, state-of-the-art HSF Simulation, and the proposed Joint HSF Simulation on various single-layer QAOA instances. Detailed specifications of the circuits are shown in Tab. II. As expected, the Schrödinger simulation’s runtime mainly depends on the number of qubits—approximately doubling with every qubit added. However, for both the standard and joint HSF simulation the runtimes are heavily influenced by the number of paths. As implied in Sec. III, if the sweet spot is missed, the exponentially growing number of paths can spoil the efficiency of standard HSF simulations, making it slower than Schrödinger simulation. The evaluated QAOA instances belong to this class for which HSF simulation is, in its original form, not a recommendable technique. However, the proposed “joint cutting” can reduce the number of paths to such an extent that it can speed up the standard HSF simulation by up to a factor $\approx 4000\times$, which, in turn, allows to outperform the Schrödinger simulation by up to a factor of $\approx 200\times$. Thus, the proposed “joint cutting” enables HSF techniques to be useful for instances for which the standard HSF procedure fails. This is also made possible by keeping the preprocessing costs for “joint cutting” low, as emphasized in Sec. IV-C. Notably, the proposed method is *always* faster than the standard HSF simulation since cascades could be found in all instances.

Finally, note that “joint cutting” can be applied to other classes of circuits as well. For instance, one could simulate deeper circuits for quantum many-body dynamics as those in [32] or join CZ or iSWAP gates in shallow instances of Google’s supremacy circuits [33]. We tested the latter but due to page limitations, these results are relegated to the aforementioned GitHub repository.

VI. CONCLUSIONS

In conclusion, this work presented a method for enhancing HSF simulation, enabling it to be faster than Schrödinger

TABLE I: Runtimes of QAOA circuits. For the runtimes, the first line is the full time with preprocessing, and the second line is only the simulation itself. Note that the preprocessing not only contains the Schmidt Decomposition and construction of paths for the “joint cutting” but also gate fusion in both cases [34], [35]. The mean of those runtimes is displayed. In brackets, one can see the standard deviation from the mean of five runs. The column S/J shows the total Schrödinger time divided by the full “joint cutting” time, and T/J the same but for the full time of standard cutting divided by the full “joint cutting” time. If the standard cutting is timed out, the lower bound of T/J is given. The bold entries display those in which the proposed method performs better. For all computations, the first 10^6 amplitudes were computed.

| Circuit | Schrödinger | Standard HSF | | Proposed Joint Cutting HSF | | Performance Ratios | |
|---------|-------------------------------------|------------------------------------|----------|----------------------------------|----------|--------------------|------------------------|
| | Runtime (s) | Runtime (s) | # Paths | Runtime (s) | # Paths | S/J | T/J |
| q30-1 | 43.177 (0.149) 42.915 (0.150) | 118.022 (2.041) 118.022 (2.041) | 2^{17} | 0.618 (0.021) 0.618 (0.021) | 2^{11} | 69.857 | 190.950 |
| q30-2 | 45.292 (0.024) 45.029 (0.026) | timed out (1 h) | 2^{26} | 1.480 (0.054) 1.444 (0.055) | 2^{12} | 30.604 | \geq 2432.544 |
| q30-3 | 46.280 (0.051) 46.018 (0.051) | timed out (1 h) | 2^{29} | 49.003 (1.648) 48.991 (1.646) | 2^{17} | 0.944 | \geq 73.465 |
| q31-1 | 91.956 (0.120) 91.435 (0.122) | 308.671 (4.552) 308.671 (4.552) | 2^{18} | 0.389 (0.050) 0.379 (0.049) | 2^{10} | 236.188 | 792.821 |
| q31-2 | 97.372 (0.056) 96.851 (0.056) | timed out (1 h) | 2^{28} | 13.874 (0.122) 13.863 (0.122) | 2^{15} | 7.018 | \geq 259.473 |
| q31-3 | 99.860 (0.051) 99.339 (0.050) | timed out (1 h) | 2^{34} | 6.670 (0.152) 6.620 (0.146) | 2^{14} | 14.971 | \geq 539.726 |
| q32-1 | 201.494 (0.039) 200.457 (0.041) | timed out (1 h) | 2^{24} | 0.848 (0.012) 0.822 (0.005) | 2^{11} | 237.692 | \geq 4246.730 |
| q32-2 | 202.769 (0.060) 201.728 (0.063) | timed out (1 h) | 2^{25} | 1.605 (0.008) 1.564 (0.007) | 2^{12} | 126.356 | \geq 2243.348 |
| q32-3 | 209.714 (0.042) 208.676 (0.042) | timed out (1 h) | 2^{30} | 3.219 (0.036) 3.165 (0.037) | 2^{13} | 65.147 | \geq 1118.324 |
| q33-1 | 427.595 (0.102) 425.519 (0.095) | timed out (1 h) | 2^{24} | 7.409 (0.264) 7.402 (0.263) | 2^{14} | 57.711 | \geq 485.879 |
| q33-2 | 435.864 (0.183) 433.787 (0.188) | timed out (1 h) | 2^{27} | 34.042 (1.109) 34.031 (1.110) | 2^{16} | 12.804 | \geq 105.751 |
| q33-3 | 463.847 (12.571) 457.035 (3.128) | timed out (1 h) | 2^{30} | 16.884 (0.100) 16.843 (0.104) | 2^{15} | 27.473 | \geq 213.221 |

TABLE II: Specifications of the QAOA circuits where the problem graphs are generated with networkx’ stochastic_block_model. The column “sizes” indicates the number of vertices per partition of the problem graph, which sum up to q and have connecting edges within the partition with probability p_{intra} and between the partitions with p_{inter} . The “cut pos.” denotes the qubit label after which the cut is performed (roughly after half the qubits q). “blocks + sep” counts the number of cut blocks and the remaining separate cuts (which could not be summarized in a block). “sep. cuts” counts the total separate cuts. The total number of 2-qubit gates in the circuit is given in column “# 2-qubit gates”. All QAOA instances contain a single problem layer and a single mixer layer.

| Circuit | q | cut pos. | # 2-qubit gates | sizes | p_{inter} | p_{intra} | blocks + sep. | sep. cuts |
|---------|----|----------|-----------------|---------|-------------|-------------|---------------|-----------|
| q30-1 | 30 | 14 | 172 | [15,15] | 0.1 | 0.8 | 5+6 | 17 |
| q30-2 | 30 | 14 | 181 | [15,15] | 0.15 | 0.8 | 6+6 | 26 |
| q30-3 | 30 | 14 | 185 | [15,15] | 0.17 | 0.8 | 7+10 | 29 |
| q31-1 | 31 | 14 | 186 | [15,16] | 0.1 | 0.8 | 6+4 | 18 |
| q31-2 | 31 | 14 | 197 | [15,16] | 0.15 | 0.8 | 8+7 | 28 |
| q31-3 | 31 | 14 | 203 | [15,16] | 0.17 | 0.8 | 9+5 | 34 |
| q32-1 | 32 | 15 | 206 | [16,16] | 0.1 | 0.8 | 6+5 | 24 |
| q32-2 | 32 | 15 | 207 | [16,16] | 0.11 | 0.8 | 5+7 | 25 |
| q32-3 | 32 | 15 | 214 | [16,16] | 0.12 | 0.8 | 7+6 | 30 |
| q33-1 | 33 | 15 | 219 | [16,17] | 0.1 | 0.8 | 6+8 | 24 |
| q33-2 | 33 | 15 | 223 | [16,17] | 0.11 | 0.8 | 6+10 | 27 |
| q33-3 | 33 | 15 | 234 | [16,17] | 0.12 | 0.8 | 8+7 | 30 |

simulation for instances, in which the standard HSF simulation would fail. This approach is effective when circuits contain identifiable blocks (e.g., cascades), making it a valuable tool for structured circuit types. However, it is important to note that, like Quantum Circuit Cutting, HSF simulation remains best suited for specific circuit shapes, with challenges still arising for deep and dense circuits—even for the enhanced “joint cutting”. While these limitations persist, our results highlight meaningful advancements in the scope and applicability of HSF techniques. Future work could explore further refinements in gate grouping for “joint cutting”. For instance, in addition to regrouping the gates, adjusting the qubit order itself may help further to identify beneficial blocks that can be cut jointly.

ACKNOWLEDGMENT

This work received funding from the European Research Council (ERC) under the European Union’s Horizon 2020 research and innovation program (grant agreement No. 101001318), was part of the Munich Quantum Valley, which the Bavarian state government supports with funds from the Hightech Agenda Bayern Plus, and has been supported by the BMWK based on a decision by the German Bundestag through project QuaST, as well as by the BMK, BMDW, and the State of Upper Austria in the frame of the COMET program (managed by the FFG).

REFERENCES

- [1] Scott Aaronson and Lijie Chen, *Complexity-theoretic foundations of quantum supremacy experiments*, Dec. 26, 2016. DOI: 10.48550/arXiv.1612.05903. arXiv: 1612.05903[quant-ph].
- [2] Igor L. Markov *et al.*, *Quantum supremacy is both closer and farther than it appears*, Sep. 26, 2018. DOI: 10.48550/arXiv.1807.10749. arXiv: 1807.10749[quant-ph].
- [3] Zhao-Yun Chen *et al.*, “64-qubit quantum circuit simulation,” *Science Bulletin*, vol. 63, no. 15, pp. 964–971, Aug. 15, 2018. DOI: 10.1016/j.scib.2018.06.007.
- [4] Michael A. Nielsen and Isaac L. Chuang, *Quantum Computation and Quantum Information: 10th Anniversary Edition*. Dec. 9, 2010, ISBN: 9780511976667 Publisher: Cambridge University Press. DOI: 10.1017/CBO9780511976667.
- [5] Danylo Lykov *et al.*, *Tensor network quantum simulator with step-dependent parallelization*, Apr. 20, 2022. DOI: 10.48550/arXiv.2012.02430. arXiv: 2012.02430[quant-ph].
- [6] Johnnie Gray and Stefanos Kourtis, “Hyper-optimized tensor network contraction,” *Quantum*, vol. 5, p. 410, Mar. 15, 2021. DOI: 10.22331/q-2021-03-15-410. arXiv: 2002.01935[cond-mat, physics:physics, physics:quant-ph].
- [7] Edwin Pednault *et al.*, *Pareto-efficient quantum circuit simulation using tensor contraction deferral*, Aug. 27, 2020. DOI: 10.48550/arXiv.1710.05867. arXiv: 1710.05867[quant-ph].
- [8] Igor L. Markov and Yaoyun Shi, “Simulating quantum computation by contracting tensor networks,” *SIAM J. Comput.*, vol. 38, no. 3, pp. 963–981, Jan. 2008. DOI: 10.1137/050644756. arXiv: quant-ph/0511069.
- [9] Lukas Burgholzer, Alexander Ploier, and Robert Wille, “Exploiting arbitrary paths for the simulation of quantum circuits with decision diagrams,” in *2022 Design, Automation & Test in Europe Conference & Exhibition (DATE)*, ISSN: 1558-1101, Mar. 2022, pp. 64–67. DOI: 10.23919/DATES4114.2022.9774631.
- [10] Lukas Burgholzer, Hartwig Bauer, and Robert Wille, “Hybrid schrödinger-feynman simulation of quantum circuits with decision diagrams,” in *2021 IEEE International Conference on Quantum Computing and Engineering (QCE)*, Oct. 2021, pp. 199–206. DOI: 10.1109/QCE52317.2021.00037.
- [11] Robert Wille, Stefan Hillmich, and Lukas Burgholzer, “Tools for quantum computing based on decision diagrams,” *ACM Transactions on Quantum Computing*, vol. 3, no. 3, pp. 1–17, Sep. 30, 2022. DOI: 10.1145/3491246. arXiv: 2108.07027[quant-ph].
- [12] Lukas Burgholzer, Alexander Ploier, and Robert Wille, *Tensor networks or decision diagrams? guidelines for classical quantum circuit simulation*, Feb. 13, 2023. DOI: 10.48550/arXiv.2302.06616. arXiv: 2302.06616[quant-ph].
- [13] Holger F. Hofmann, “How to simulate a universal quantum computer using negative probabilities,” *J. Phys. A: Math. Theor.*, vol. 42, no. 27, p. 275304, Jun. 2009. DOI: 10.1088/1751-8113/42/27/275304.
- [14] Tianyi Peng *et al.*, “Simulating large quantum circuits on a small quantum computer,” *Phys. Rev. Lett.*, vol. 125, no. 15, p. 150504, Oct. 6, 2020. DOI: 10.1103/PhysRevLett.125.150504. arXiv: 1904.00102[quant-ph].
- [15] Kosuke Mitarai and Keisuke Fujii, “Overhead for simulating a non-local channel with local channels by quasiprobability sampling,” *Quantum*, vol. 5, p. 388, Jan. 28, 2021. DOI: 10.22331/q-2021-01-28-388.
- [16] Christophe Piveteau and David Sutter, “Circuit knitting with classical communication,” *IEEE Trans. Inform. Theory*, vol. 70, no. 4, pp. 2734–2745, Apr. 2024. DOI: 10.1109/TIT.2023.3310797. arXiv: 2205.00016[quant-ph].
- [17] Christian Ufrecht *et al.*, “Cutting multi-control quantum gates with ZX calculus,” *Quantum*, vol. 7, p. 1147, Oct. 23, 2023. DOI: 10.22331/q-2023-10-23-1147.
- [18] Christian Ufrecht *et al.*, “Optimal joint cutting of two-qubit rotation gates,” *Phys. Rev. A*, vol. 109, no. 5, p. 052440, May 30, 2024. DOI: 10.1103/PhysRevA.109.052440.
- [19] Lukas Schmitt, Christophe Piveteau, and David Sutter, *Cutting circuits with multiple two-qubit unitaries*, Apr. 26, 2024. DOI: 10.48550/arXiv.2312.11638. arXiv: 2312.11638[quant-ph].
- [20] Marvin Bechtold *et al.*, “Investigating the effect of circuit cutting in QAOA for the MaxCut problem on NISQ devices,” *Quantum Sci. Technol.*, vol. 8, no. 4, p. 045022, Sep. 2023, Publisher: IOP Publishing. DOI: 10.1088/2058-9565/acf59c.
- [21] Hiroyuki Harada, Kaito Wada, and Naoki Yamamoto, *Doubly optimal parallel wire cutting without ancilla qubits*, Nov. 7, 2023. DOI: 10.48550/arXiv.2303.07340. arXiv: 2303.07340[quant-ph].
- [22] Angus Lowe *et al.*, “Fast quantum circuit cutting with randomized measurements,” *Quantum*, vol. 7, p. 934, Mar. 2, 2023. DOI: 10.22331/q-2023-03-02-934.
- [23] Marvin Bechtold *et al.*, *Joint wire cutting with non-maximally entangled states*, Jun. 19, 2024. DOI: 10.48550/arXiv.2406.13315. arXiv: 2406.13315[quant-ph].
- [24] Michael A. Nielsen *et al.*, “Quantum dynamics as a physical resource,” *pra*, vol. 67, no. 5, 052301, p. 052301, 2003. DOI: 10.1103/PhysRevA.67.052301. arXiv: quant-ph/0208077 [quant-ph].
- [25] Quantum AI team and collaborators, *Qsim*, 2020. DOI: 10.5281/zenodo.4023103.
- [26] Frank Arute *et al.*, “Quantum supremacy using a programmable superconducting processor,” *Nature*, vol. 574, no. 7779, pp. 505–510, Oct. 2019, Publisher: Nature Publishing Group. DOI: 10.1038/s41586-019-1666-5.
- [27] Peter L. Ivănescu, “Some network flow problems solved with pseudo-boolean programming,” *Operations Research*, vol. 13, no. 3, pp. 388–399, 1965. DOI: 10.1287/opre.13.3.388. eprint: <https://doi.org/10.1287/opre.13.3.388>.
- [28] F. Barahona, M. Jünger, and G. Reinelt, “Experiments in quadratic 0–1 programming,” *Mathematical Programming*, vol. 44, no. 1–3, pp. 127–137, 1989. DOI: 10.1007/bf01587084.
- [29] Caterina De Simone, “The cut polytope and the boolean quadric polytope,” *Discrete Mathematics*, vol. 79, no. 1, pp. 71–75, 1990. DOI: 10.1016/0012-365x(90)90056-n.
- [30] Michael Jünger and Sven Mallach, “Exact facetial odd-cycle separation for maximum cut and binary quadratic optimization,” *INFORMS Journal on Computing*, 2021. DOI: 10.1287/ijoc.2020.1008.
- [31] Laura S. Herzog *et al.*, *Improving quantum and classical decomposition methods for vehicle routing*, Apr. 8, 2024. DOI: 10.48550/arXiv.2404.05551. arXiv: 2404.05551[quant-ph].
- [32] Jonas Richter, *Simulating the dynamics of large many-body quantum systems with schrödinger-feynman techniques*, Mar. 28, 2024. DOI: 10.48550/arXiv.2403.19864. arXiv: 2403.19864[cond-mat, physics:quant-ph].
- [33] Sergio Boixo and Charles Neill. “The question of quantum supremacy.” <https://github.com/sboixo/GRCS>. ()
- [34] Mikhail Smelyanskiy, Nicolas P. D. Sawaya, and Alán Aspuru-Guzik, “qHiPSTER: The Quantum High Performance Software Testing Environment,” *arXiv e-prints*, arXiv:1601.07195, arXiv:1601.07195, 2016. DOI: 10.48550/arXiv.1601.07195. arXiv: 1601.07195 [quant-ph].
- [35] Thomas Häner and Damian S. Steiger, “0.5 Petabyte Simulation of a 45-Qubit Quantum Circuit,” *arXiv e-prints*, arXiv:1704.01127, arXiv:1704.01127, 2017. DOI: 10.48550/arXiv.1704.01127. arXiv: 1704.01127 [quant-ph].